

# Breaking atomic nuclei into little pieces: Evidence for a phase transition

W. Bauer\*, M. Kleine Berkenbusch, and T. Bollenbach

*National Superconducting Cyclotron Laboratory and Department of Physics and Astronomy,  
Michigan State University, East Lansing,  
MI 48824-2320, USA,  
e-mail: bauer@pa.msu.edu*

Recibido el ?? de ?? de ??; aceptado el ?? de ?? de ??

Recent data obtained for the fragmentation of gold nuclei after bombardment with high energy protons at the BNL-AGS shows that it is possible to generate conditions in finite nuclei that are sufficiently close to the critical point of the nuclear matter phase diagram. We have compared these data to theoretical models based on the percolation universality class and find excellent agreements. Based on this, we conclude that there now is conclusive evidence for a continuous phase transition in nuclear fragmentation.

*Keywords:* FAVOR DE PROPORCIONAR

Datos recientes obtenidos para la fragmentación de los núcleos del oro después de el bombardeo con protones de alta energía en el BNL-AGS muestra que es posible generar condiciones en los núcleos finitos que están suficientemente cerca del punto crítico del diagrama de fase de la materia nuclear. Hemos comparado estos datos a los modelos teóricos basados en la clase de la universalidad de la filtración y encontramos acuerdos excelentes. De acuerdo con esto, concluimos que ahora hay evidencia concluyente para una transición continua de la fase en la fragmentación nuclear.

*Descriptores:* FAVOR DE PROPORCIONAR

PACS: 24.60.-k; 25.70.Pq; 25.80.Hp

## 1. Basic Questions

The search for thermodynamic phase transitions in excited nuclear systems has been one of the main motivations for heavy ion research during the last two decades. The fragmentation transition and the quark-gluon plasma transition are the two most likely candidates for a successful conclusion of these searches. The fragmentation phase transition between the nuclear Fermi liquid and a hadron gas has been studied longer, and its properties now are fairly well constrained. We now believe that the transition is of first order, terminating at a critical point. The properties of this critical point are, of course, of paramount interest in this area of research. This line of investigation enables us to make connections between our research results in nuclear physics and our everyday experiences with systems that undergo phase transitions, like for example liquid water turning into ice or steam.

However, while the analogy to the evaporation of water is tantalizing, there are very basic questions that need to be asked before we can convince ourselves that even drawing such a diagram makes sense. These questions include: Can one provide reliable measurements of the thermodynamic state variables? Is thermodynamic equilibrium ever established? Can we prepare a state at a certain point in the phase diagram? Can one talk of a phase transition in a system with only  $10^2$  to  $10^3$  constituents? And how do final state interactions and sequential decays influence our ability to make conclusions regarding the cluster size distribution at the phase transition point?

So let us discuss some of the answers to these questions! It is obvious that we as nuclear physicists have to live without

direct observations of the nuclear reactions we are interested in. The time scales and length scales are simply too small for us to hope that this will ever change. We are thus relegated to restricting our measurements to the asymptotic momentum states of particles emitted from the reaction zone. However, interferometry of the Hanbury-Brown-Twiss type provides us with information on the reaction volume and thus the density. And several thermometers have been developed to aid us in measuring the temperature.

As for the question regarding the establishment of thermodynamic equilibrium: We have indirect evidence that this is indeed the case. Thermal model description have been incredibly successful in providing predictions for particle production rates, energy spectra, and so forth, starting with the "fireball" model [1, 2]. Of course one may argue that one also performs ensemble averages when one compares thermal models to data, and that ensemble averaging can produce results similar to thermal averaging. However, recently the large acceptance of the STAR detector at RHIC and the large numbers of particles emitted in individual Gold-Gold collisions have enabled us to look at thermal quantities in individual events. And they establish that at least in these collisions a thermal description seems to be warranted.

The question regarding the preparation of a state at a fixed point in the phase diagram has to be answered with 'no'. In any given individual heavy ion collision the colliding system migrates through the phase diagram. In addition, the shape of the reaction zone for symmetric heavy ion collisions changes greatly during the course of the event. This question can thus not be answered in general terms. However, numerical studies indicate that at least for the fragmentation phase transition

the fragment size distribution and its moments are determined mainly in the vicinity of the critical point, if the system passes sufficiently close to that point.

And, finally, regarding the finite size: While we cannot expect the divergences that one sees in the thermodynamic limit, we can still see finite size remnants of them in the data. This can best be shown with the aid of a phase transition model that has a well-understood infinite size limit, but that can be applied for finite size systems. Scaling arguments that introduce a scaling exponent  $\nu$  and multiply the control parameter by  $L^{1/\nu}$  and the order parameter by  $L^{\beta/\nu}$  are usually employed to extrapolate from finite lattice size  $L$  to the infinite size limit. In nuclear physics the extreme finite size limit can also be accessed. And thus the small number of constituents is not a shortcoming, but instead provides valuable insights into the applicability of finite size scaling ideas.

We will discuss the role of sequential decays more explicitly in the following sections.

## 2. Percolation-based model for the phase transition

One class of models that have a well-defined infinite size limit, a continuous phase transition with known critical exponents, and that can be applied to finite systems with exact particle number conservation are those based on percolation theory [3–10].

Percolation models come in site- or bond-percolation or mixed variants. We are going to concentrate on bond-percolation approaches, in which nucleons are represented by lattice sites, and their (short-range) interactions are represented by bonds. All physically relevant parameters, such as the critical exponents, do not depend on the lattice structure, only on the dimensionality. Even random lattices deliver essentially the same results.

The bonds in our nuclei can be broken with a certain probability, which serves as the control parameter of the phase transition. Connecting the bond breaking probability with the physical parameters of the system usually assumes global equilibrium and contains most of the physics that enters this problem. It is also at this point where quantum mechanics enters in a fundamental way into our model. One can incorporate the influence of the impact parameter in proton or other light particle induced reactions in the limiting fragmentation region ( $E_{\text{beam}} > 10$  GeV), for example, through the use of the eikonal approximation. For nucleus-nucleus collisions, we have to resort to more complicated integrations and usually have to employ calculations with transport models to implement the energy deposition.

In physical systems of relevance in our field, we usually have to deal with the fact that there is more than one species present. However, one can show [11] that for all physical choices of the control parameters this problem can be reduced to that of a one-component percolation system.

Percolation models have been successful in reproducing fragment mass distributions, fragment energy spectra, dependence of the moments of the fragment distribution on multiplicity, fragment-fragment correlations, size of the largest fragment (a measure for the order parameter) as a function of multiplicity (an approximate measure for the control parameter). In Fig. 1 we show the experimental [12–14] and theoretical [15, 16] charge yield spectra for the reaction 10.8 GeV  $\pi + \text{Au}$ .

Shown here are the results from a total of 500,000 completely reconstructed events, *i.e.* events in which all charges were accounted for. For the theoretical calculations, this is of course not a problem at all. For the experimental data, however, it constitutes a very strong statement. All fast and slow emitted IMFs ( $Z_f \leq 3$ ) and light particles (He- and H-isotopes) were accounted for. However, the big evaporation residue was stopped by the target frame and thus not observable. So the assumption that all not detected charges were part of the residue fragment is inherent in the presentation of the data. For the inclusive charge yield spectra, this is not at all a problem. However, when one investigates moments of the charge yield spectra, of fluctuations, this assumption becomes questionable.

Note that Fig. 1 contains two theory curves, those that were unfiltered, and those that were passed through the software filters representing the detection efficiencies and detector geometries, as well as sequential decay corrections [17, 18]. These sequential decay corrections were found to be essential, in particular if one wants to make statements on the isospin dependence of the nuclear equation of state [19].

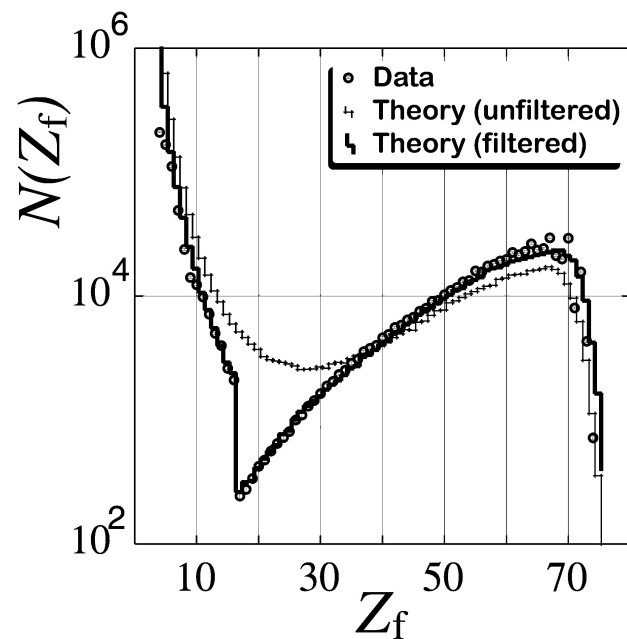


FIGURE 1. Charge yields from the reaction 10.8 GeV  $\pi + \text{Au}$ . Circles: ISiS data [12–14], thin histogram: unfiltered calculations, thick histogram: filtered and decay corrected calculations.

As one can observe, the agreement between data and filtered calculations for the inclusive charge yield spectra presented in Fig. 1 is almost perfect. This is an indication that the theory does well in reproducing the experimental data, and that we understand all of the detector and sequential decay corrections.

Figure 2 shows the percolation model calculations for the energy spectra of  $^{12}\text{C}$  spectra (circles) and compares to experiment [20] (histogram) for the reaction  $300\text{ GeV p} + \text{Xe}$ . Here, Coulomb trajectory calculations are employed beyond the freeze-out density. This sets a volume scale in the model, even though the pure bond percolation model does not have the density as a control parameter. Best agreement with data is reached for  $\rho = 0.36 \rho_0$ . One should note that the slope temperature of the fragments shown here is approximately  $12\text{ MeV}$ , much higher than the intrinsic temperature. This is a consequence of the fermionic nature of the nucleons that are contained in these fragments and their zero-point motion (See also [21] for a more detailed explanation of this point).

For both Figs., 1 and 2, we performed integrations over all impact parameters and the corresponding event classes, with their proper weights, to reproduce the inclusive experimental data sets. These two figures lend credibility to the claim that the model reproduces all inclusive data for production cross sections and energy distributions of fragments of all sizes.

It is interesting that a similar percolation approach, with a different lattice dimension and geometry, as well as a different method for energy deposition, is able to reproduce the fragmentation cross section of buckyballs (C-60 molecules) into carbon clusters of different sizes [22, 23]. Cross-disciplinary comparisons between these two different reaction types reveal stunning similarities, such as the U-shape of the fragments production spectrum, a power-law fall off for small to medium mass cluster production cross sections, and modifications to sequential decays and binding energy effects.

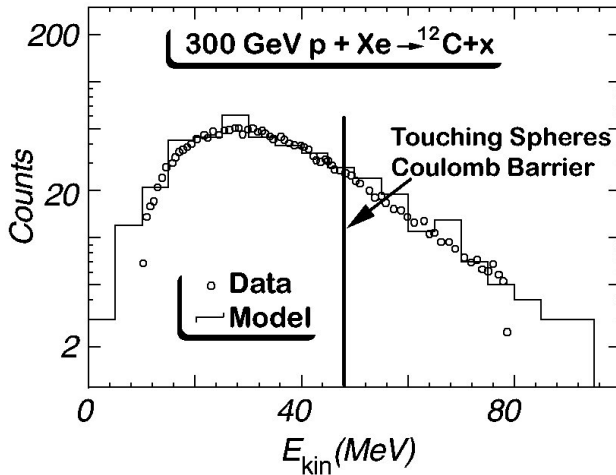


FIGURE 2. Comparison of the experimental data for the energy spectra of  $^{12}\text{C}$  from the fragmentation reaction  $300\text{ GeV p} + \text{Xe}$  (histogram) [20] with the result of the percolation model with Coulomb expansion and a freeze-out density of  $\rho = 0.36 \rho_0$ .

### 3. Scaling

We now turn our attention to exclusive events and employ event by event (EbyE) analysis techniques. EbyE techniques are needed, if one aims to investigate fluctuations, because conventional averaging procedures may destroy information on fluctuations.

On such EbyE procedure focuses on the moments of the cluster size distribution. In Ref. [8, 9] we have shown that the data of the EoS-TPC collaboration [24, 25] for the second moment of the cluster size distribution in  $1\text{ AGeV Au} + \text{C}$  collisions can be reproduced by a percolation based model, and that a subset of the experimental events probed a region sufficiently close to the critical point. In a comparison to the ISiS-BNL data [13, 14] we reached similar conclusions in Ref. [15, 16].

From analytical solutions and numerical results, it can be inferred that in percolation theory, for the control parameter  $p$  assuming values close to the critical value  $p_c$ , the cluster numbers behave as follows:

$$N(s(p)) = s^{-\tau} f[(p - p_c)s^\sigma] \quad (\text{for } p \approx p_c) \quad (1)$$

where  $s$  is the cluster size. (For the purpose of our nuclear fragmentation experiments, where only the charge of the fragment is detected, we use this charge  $Z_f$  as the cluster size parameter.) The scaling function  $f$  is "close" to an exponential, has the property  $f(0) = 1$ , and accounts for the fact that a power law dependence is only correct in the case of  $p = p_c$ . One can see from this equation that when one divides both sides by the power-law term and takes the logarithm, one should expect a straight line when plotting  $\log(\langle N(Z_f)/q_0 Z_f^{-\tau} \rangle)$  vs.  $\epsilon Z_f^\sigma$  in the vicinity of the critical point, where this scaling behavior holds.  $\epsilon$  is here the dimensionless control parameter,

$$\epsilon = \frac{p_c - p}{p} \quad (2)$$

(or  $\epsilon = (T_c - T)/T$ , if the temperature is selected as the control parameter).

In addition, the straight line in the plot of the scaled yield versus the scaled control parameter should have the property of  $f(0) = 1$  [26–28]. This scaling behavior close to the critical point is typical for basically all known theories.

We are now able to treat the critical exponents  $\sigma$  and  $\tau$ , as well as the critical value of the breaking probability  $p_c$  (or critical temperature  $T_c$ ) as parameters in a  $\chi^2$  optimization procedure. If we correct the experimental data for sequential decays, then we find that both, experiment and theory, collapse onto a universal curve that passes through the point  $(0, 1)$  in the plot of the log of the reduced yield vs. the reduced control parameter. This is shown in Fig. 3 and is the strongest evidence yet for the experimental observation of the critical point of the fragmentation phase transition.

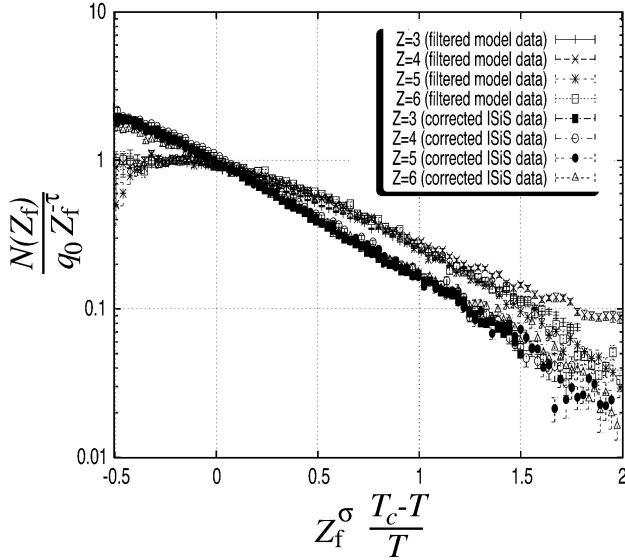


FIGURE 3. Comparison of the experimental and theoretical scaling collapse of the fragmentation cross section for different charged fragments at different values of the control parameter.

We should note that for this figure we have converted the theoretical breaking probability into an equivalent temperature by using [10] the relationship

$$p_b(T) = 1 - \frac{2}{\sqrt{\pi}} \Gamma\left(\frac{3}{2}, 0, \frac{B}{T}\right), \quad (3)$$

where  $\Gamma$  is the generalized incomplete gamma function,  $B$  is the binding energy per nucleon in the residue (taken as 6 MeV here), and  $T$  is the temperature. This prescription is a generalization of the Coniglio-Klein formula for the existence of a bond between neighboring sites [29, 30]

$$p_{CK} = 1 - \exp(-\mathcal{E}/2T) \quad (4)$$

where  $\mathcal{E}$  is the nearest-neighbor interaction energy. Thus there is a close connection between the bond percolation theory and the lattice gas model.

The output of the  $\chi^2$  optimization procedure also gives us the best values for the critical temperature and critical exponents. For the theory, this procedure yields  $\sigma = 0.45$ ,  $\tau = 2.18$ , and  $T_c = 9.2$  MeV (corresponding to  $p_c = 0.7$ ). The critical exponents are close to those calculated for "infinite" size percolation systems. And the critical value of the control parameter shows the well-known [3] finite size corrections. The extracted parameters for the experiment are  $\sigma = 0.5 \pm 0.1$ ,  $\tau = 2.35 \pm 0.05$ , and  $T_c = 8.3 \pm 0.2$  MeV.

It is absolutely essential for this scaling collapse to possible that the effects of sequential decay corrections and final state interactions, as well as those of detector inefficiencies, are removed from the experimental data. We accomplish this by subjecting our calculations to all of these effects and running them through a software representation of the detector acceptance. Then we compare the unfiltered and uncorrected results of our calculations to the filtered and decay-corrected.

From this comparison, we extract element-by-element correction factors for each temperature that we apply to the experimental data. The validity of this correction scheme is strengthened by the excellent agreement between filtered and decay-corrected calculations and experimental data, as shown in Fig. 1. Again, without these careful corrections for sequential decays and detector acceptance a scaling collapse cannot be achieved, and the analysis we have employed would be meaningless.

We should add at this point that Elliott *et al.* [28] have reached similar conclusions to ours, employing a similar scaling analysis technique, but a much more simplified treatment of the sequential decays. Within the error bars, the set of critical exponents that they report agrees well with ours. However, they find a critical temperature of 6.7 MeV, somewhat lower than the result of our analysis. The group of Gulinelli *et al.* [31] has used their lattice gas model for a similar scaling analysis as well. They have observed scaling for subcritical as well as critical values in their model, which has the two control parameters density and temperature.

We finish our discussion of the scaling analysis with two words of caution. Of course a scaling analysis is attractive, because it can give hints of scale invariance as expected near the critical point of a continuous phase transition, and because it can help us to determine the universality class of that transition. However, in finite systems the number of constituents provides an inherent scale that will necessarily result in a cut-off for this scaling. In our case, this is the reason that we cannot expect any scaling behavior that spans more than two orders of magnitude.

Also, there are other scenarios that can lead to scaling behavior. Most promising among the recently discussed is self-organized criticality. Here, the ingredients that lead to scale invariance are a feedback loop of slow steady infusion of stress on a system, coupled with fast avalanche-like releases of this stress. For a further discussion of this class of scenario, as well as an instructive simple example, we refer to [32].

Thus we cannot hope for a proof of scaling from the experimental data alone. Rather we are relegated to comparisons with theories of known universality classes in the infinite size limit, such as for example the percolation model. Agreement of the data with the finite size implementation can then, in the best case, provide circumstantial evidence for the existence and properties of the phase transition. This is what we are arguing here.

#### 4. Size and size fluctuations of the largest cluster

The size of the largest cluster serves as the order parameter in the phase transition. One expects the order parameter near the critical value of the control parameter to decay according to  $(p - p_c)^\beta$ , with the fluctuations in the order parameter reaching a maximum.

The fluctuations (variance) in the size of the largest fragment support the conclusions we have reached above. In Fig. 4, lower panels, we show the theoretical calculations and experimental data for the average size of the largest fragment,  $Z_{\max}$  in each event, binned by the excitation energy or, equivalently, the breaking probability in each event. Since we thus know the average of this quantity, and since we also have this information on an event by event basis, we can then extract the variance of  $Z_{\max}$  as well,  $Var(Z_{\max})$ . This is shown in the upper two panels of Fig. 4.

One can see in the upper left panel of Fig. 4 that the variance in the size of the largest fragment has a maximum near the value of 0.7 for the order parameter, in accordance with the results of the  $\chi^2$  optimization procedure for the scaling exponents reported above. A similar peak is observed in the upper right panel for the experimental data, for an excitation energy of 5 MeV. Converting this value of an excitation energy to an equivalent temperature via, for example, a Fermi gas formula ( $E^* = aT^2$ ) again locates this maximum of the variance of the largest fragment size close to the value of the critical temperature extracted for the experimental data in the  $\chi^2$  optimization procedure that led to the results contained in Fig. 3.

## 5. Conclusions

We have extracted the value of the critical temperature as well as those of the critical exponents  $\sigma$  and  $\tau$  from experimental data. The best values are  $\sigma = 0.5 \pm 0.1$ ,  $\tau = 2.35 \pm 0.05$ , and  $T_c = 8.3 \pm 0.2$  MeV. These are very close to those expected from models based on the percolation universality class, once finite scaling effects are taken into account. Additionally, our percolation-based model is able to reproduce a wide array of experimental data on fragment yields, event by event moments of the size distribution, scaling, and size and fluctua-

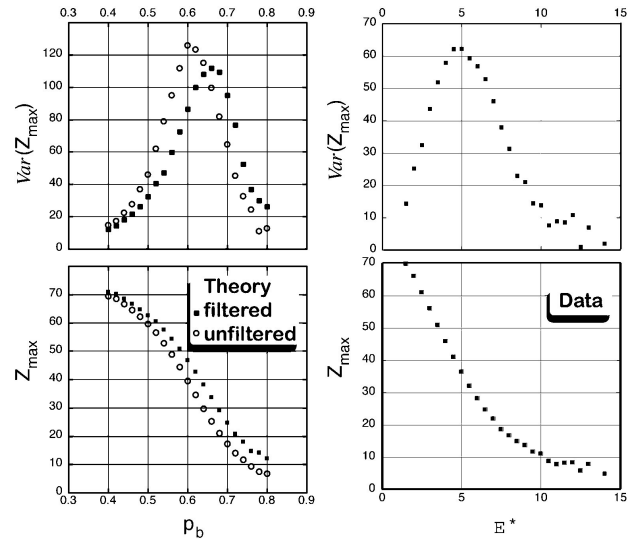


FIGURE 4. Comparison of the theoretical predictions (left two panels) to the experimental data (right two panels) for the size of the largest fragment (lower panels) and the variance in this quantity (upper two panels). For the theory, both the unfiltered (open symbols) and filtered (filled symbols) results are shown.

tions of the largest cluster. These are strong indications that the critical point has been located, and its properties determined. The universality class of the nuclear fragmentation phase transition appears to be that of the percolation type.

## Acknowledgements

This work was supported by NSF grants INT-9981342 and PHY-0070818, the Studienstiftung des Deutschen Volkes (MKB, TB), and an Alexander-von-Humboldt Foundation Distinguished Senior U.S. Scientist Award (WB). Collaborations with Vic Viola, Luc Beaulieu and their experimental group in the analysis of their data are very much appreciated.

\*. URL: <http://www.pa.msu.edu/~bauer/>

1. G.D. Westfall *et al.*, *Phys. Rev. Lett.* **37** (1976) 1202.
2. J. Gosset, J. Kapusta, and G.D. Westfall, *Phys. Rev. C* **18** (1978) 844.
3. W. Bauer, D.R. Dean, U. Mosel, and U. Post, *Phys. Lett. B* **150** (1985) 53.
4. W. Bauer, U. Post, D.R. Dean, and U. Mosel, *Nucl. Phys. A* **452** (1986) 699.
5. X. Campi, *J. Phys. A* **19** (1986) L917.
6. T.S. Biro, J. Knoll, and J. Richert, *Nucl. Phys. A* **459** (1986) 692.
7. J. Nemeth, M. Barranco, J. Desbois, and C. Ngo, *Z. Phys. A* **325** (1986) 347.
8. W. Bauer and A. Botvina, *Phys. Rev. C* **52** (1995) R1760.
9. W. Bauer and A. Botvina, *Phys. Rev. C* **55** (1997) 546.
10. T. Li *et al.*, *Phys. Rev. Lett.* **70** (1993) 1924.
11. H.M. Harreis and W. Bauer, *Phys. Rev. B* **62** (2000) 8719.
12. T. Lefort *et al.*, *Phys. Rev. Lett.* **83** (1999) 4033.
13. L. Beaulieu *et al.*, *Phys. Lett.* **B163** (1999) 159.
14. L. Beaulieu *et al.*, *Phys. Rev. C* **63** (2001) 031302.
15. W. Bauer *et al.*, *Heavy Ion Physics* **15** (2001) 217.
16. M. Kleine Berkenbusch *et al.*, *Phys. Rev. Lett.* **88** (2002) 022701.
17. S. Pratt, W. Bauer, Ch. Morling, and P. Underhill, *Phys. Rev. C* **63** (2001) 034608.
18. W. Bauer, S. Pratt, Ch. Morling, and P. Underhill, *Heavy Ion Physics* **14** (2001) 29.
19. B.-A. Li, C.M. Ko, and W. Bauer, *Int. J. Mod. Phys. E* **7**(2) (1998) 147.

20. AS. Hirsch *et al.*, *Phys. Rev. C* **29** (1984) 508.
21. W. Bauer, *Phys. Rev. C* **51** (1995) 803.
22. T. LeBrun *et al.*, *Phys. Rev. Lett.* **72** (1994) 3965.
23. S. Cheng *et al.*, *Phys. Rev. A* **54** (1996) 3182.
24. M.L. Gilkes *et al.*, *Phys. Rev. Lett.* **73** (1994) 1590.
25. H. G. Ritter *et al.*, *Nucl. Phys. A* **583** (1995) 491c.
26. J.B. Elliott *et al.*, *Phys. Rev. Lett.* **85** (2000) 1194.
27. C.M. Mader, A. Chappars, J.B. Elliott, L.G. Moretto, L. Phair, and G.J. Wozniak, preprint nucl-th/0103030 (2001).
28. J.B. Elliott *et al.*, *Phys. Rev. Lett.* **88** (2002) 042701.
29. A. Coniglio and Klein, *J. Phys. A* **13** (1980) 2775.
30. X. Campi, X. and H. Krivine, *Nucl. Phys. A* **620** (1997) 46.
31. F. Gulminelli, Ph. Chomaz, M. Bruno, and M. D'Agostino, *Phys. Rev. C* **65** (2002) 051601.
32. W. Bauer and S. Pratt, *Phys. Rev. E* **54** (1996) R1009.